IJMS
Vol 49, No 10, October 2024

Original Article

Exploring Differentially Expressed Genes and Immune Modulation in Diffuse Large B-Cell Lymphoma through RNA Sequencing Analysis

Nor Adzimah Johdi[1], PhD; Amanda Seng[2], PhD; Wei-Kang Lee[2], PhD; Hanif Zulkhairi Mohamad Said[1], Dip MLT; Wan Fariza Wan Jamaluddin[3], MD

[1]UKM Medical Molecular Biology Institute, Universiti Kebangsaan Malaysia, Cheras, Kuala Lumpur, Malaysia;
[2]Codon Genomics Sdn Bhd, Seri Kembangan Selangor Darul Ehsan, Malaysia;
[3]Cell Therapy Center, Universiti Kebangsaan Malaysia, Cheras, Kuala Lumpur, Malaysia

Correspondence:
Nor Adzimah Johdi, PhD;
UKM Medical Molecular Biology Institute, Universiti Kebangsaan Malaysia, Cheras, Postal code: 56000,Kuala Lumpur, Malaysia
Tel: +60 3 91719065
Email: adzimah@ppukm.ukm.edu.my, adzimahjohdi@gmail.com
Received: 17 September 2023
Revised: 29 October 2023
Accepted: 19 November 2023

Abstract

Background: Diffuse large B-cell lymphoma (DLBCL) is globally recognized as the most prevalent and aggressive subtype of non-Hodgkin lymphoma. While conventional treatments are effective initially, the disease can become resistant or relapse over time. This study aimed to examine the differentially expressed genes at the transcriptome level and molecular pathways in DLBCL patients.

Methods: This investigation utilized RNA sequencing analysis to compare differentially expressed gene samples from five diffuse large B-cell lymphoma patients with two healthy volunteers. These participants were admitted to UKM Medical Center, Kuala Lumpur between 2019 and 2020. The differentially expressed genes were identified using the DESeq2 R package (version 1.10.1) using a negative binomial distribution model. The obtained P values were corrected with the Benjamin and Hochberg method and identified using a False Discovery Rate threshold of <0.05, with $\log_2$ fold change (FC) of ≥ 2 or ≤ -2.

Results: Results showed 73 differentially expressed genes between the two groups, among which 70 genes were downregulated, and three genes were upregulated. The differentially expressed genes analyzed with the Reactome pathway were significantly associated with the downregulation of antimicrobial humoral response ($P<0.001$), neutrophil degranulation ($P<0.001$), chemokine receptors bind chemokines ($P=0.028$), defensins ($P=0.028$) and metabolism of angiotensinogen ($P=0.040$).

Conclusion: These findings suggest that the identified pathways may contribute to cancer progression and weaken the immune response in diffuse large B-cell lymphoma patients. This study offers fresh insights into previously undiscovered downstream targets and pathways modulated by diffuse large B-cell lymphoma.

Please cite this article as: Johdi NA, Seng A, Lee WK, Mohamad Said HZ, Wan Jamaluddin WF. Exploring Differentially Expressed Genes and Immune Modulation in Diffuse Large B-Cell Lymphoma through RNA Sequencing Analysis. Iran J Med Sci. 2024;49(10):652-660. doi: 10.30476/IJMS.2023.100149.3234.

Keywords ● Diffuse large B-cell lymphoma ● RNA sequencing ● Gene ontology ● Transcriptome ● Immunity

What's Known

- The immune landscape in lymphoma comprises a diverse milieu of immune cells such as T cells, B cells, and macrophages, interacting with malignant lymphocytes. Immune checkpoints, cytokines, and genetic alterations influence responses.
- Immunotherapies, targeting these dynamics, show promise in enhancing anti-lymphoma immunity and improving treatment outcomes.

What's New

- There were 73 differentially expressed genes between diffuse large B-cell lymphoma patients and healthy controls, with 70 downregulated and three upregulated genes.
- Antimicrobial humoral response, neutrophil degranulation and activation, chemokine response, and defensins pathways were significantly downregulated.

Introduction

Cancer of the lymphatic system, lymphoma, can be categorized into two primary types: Hodgkin lymphoma (HL) and non-Hodgkin lymphoma (NHL). NHL is the most common type and the 10th most diagnosed cancer globally.[1] The incidence of NHL was

544,352 cases in 2020 worldwide, accounting for 1.35% of all cancer cases reported.[1] This is predicted to increase significantly each year. Lymphoma is a condition characterized by uncontrolled growth and multiplication of lymphocytes, a type of white blood cell. These cancerous lymphocytes can spread to various parts of the body such as the lymph nodes, spleen, bone marrow, blood, or other organs, forming a tumor mass. Two primary types of lymphocytes can transform into lymphomas: B lymphocytes (B cells) and T lymphocytes (T cells). B-cell lymphomas are significantly more prevalent than T-cell lymphomas and makeup roughly 85% of all NHLs.[2] The most prevalent type of NHL is diffuse large B-cell lymphoma (DLBCL), which represents around 30% of newly diagnosed NHL cases globally.[1] DLBCL affects both genders, with a slightly higher incidence in men. While it can manifest in childhood, its occurrence generally rises with age, and approximately half of those diagnosed are 60 years old or older. DLBCL is a fast-progressing form of lymphoma that can develop in the lymph nodes or outside the lymphatic system, including the gastrointestinal tract, testes, thyroid, skin, breast, bone, or brain. Because of its rapid advancement, DLBCL typically demands immediate medical intervention. In some patients suffering from this type of lymphoma, a combination of chemotherapy (cyclophosphamide, doxorubicin, vincristine, and prednisone) and the monoclonal antibody rituximab (R-CHOP), with or without radiation therapy, can result in remission of the disease.[3]

R-CHOP, administered in 21-day cycles, is the primary treatment for DLBCL and is typically the first course of action. While the initial treatment proves effective for certain patients, however, some patients may encounter disease relapse or develop refractory disease over time.[4] One-third of patients still die from the disease. Therefore, understanding the molecular mechanisms that lead to the progression of the disease is crucial for tackling this problem effectively. Clinical studies have been utilizing ribonucleic acid sequencing (RNA-Seq) more frequently to identify alterations in gene expression.[5] The RNA-Seq gene expression profile is commonly employed to incorporate various molecular events and mechanisms linked to the advancement of cancer. RNA-Seq has transcended the boundaries of the genomics community and has become a conventional research tool. This approach can serve various purposes, such as accurately detecting differentially expressed genes (DEGs). Additionally, RNA-Seq can facilitate the analysis of gene co-expression networks, pathways involved, and protein-to-protein interactions. Moreover, this established and efficient screening method can be utilized to discover novel biomarkers and enhance our comprehension of cancer biology.[6]

Transcriptome analysis enables an unbiased screening of molecular alterations that take place in DLBCL compared to normal samples, facilitating the identification of target genes and pathways. The results have the potential to guide the development of new alternative treatment strategies that focus on pathways modulated in DLBCL. The aim of this study was to examine the DEGs at the transcriptome level and tumor-promoting molecular pathways implicated in DLBCL patients in comparison with normal healthy volunteers using RNA-Seq analysis.

Patients and Methods

The research conducted followed the established protocols of the UKM Research Ethics Committee (UKM PPI/111/8/JEP-2016-063). This involved acquiring ethical clearance and written consent. Before being included in the study, all participants who contributed samples gave informed consent.

Patients

Ten mL of blood samples from five primary DLBCL patients and two normal healthy volunteers who were admitted to UKM Medical Center, Kuala Lumpur, were recruited in this study according to the rules and regulations stated. The cases were histologically confirmed and diagnosed. Normal healthy volunteers were patients who came for annual screening and were diagnosed as healthy without any underlying disease.

Peripheral Blood Mononuclear Cell (PBMC)

Each patient donated 10 mL of fresh blood, which was collected in heparin tubes from BD Vacutainer™ (Beckton Dickinson, USA). After collection, the samples were kept at 4 °C until the PBMCs were isolated, which took place within 24 hours. The isolation was performed using Ficoll Paque PLUS™ density gradient media (GE Healthcare, USA) according to the manufacturer's instructions. Subsequently, the cells were cryopreserved in a 10% dimethyl sulfoxide (DMSO) solution and stored in a liquid nitrogen tank at a temperature of -196 °C until required.

Ribonucleic acid (RNA) Extraction

To extract RNA from PBMC, the RNeasy® Mini Kit (QIAGEN, Germany) was used

following the manufacturer's instructions. The concentration and purity of the extracted RNA were measured using a NanoDrop ND-2000C spectrophotometer (Thermo Scientific, USA), and its quality was assessed using the Agilent 2100 bio-analyser system. Samples that exhibited RNA concentrations exceeding 50 ng/μL, purity A260/A280 ratios ranging in the range of 1.80 to 2.20, and RNA integrity number (RIN) values greater than seven were chosen for additional analysis, on the condition that they demonstrated undamaged RNA devoid of any deoxyribonucleic acid (DNA) or protein contamination.

Library Preparation for Transcriptome Sequencing

To prepare the RNA samples for sequencing, 1.3 μg of the total RNA was utilized as the input material. The NEBNext Ultra RNA Library Preparation Kit (New England Biolabs, Inc., USA) was utilized following the manufacturer's instructions to create sequencing libraries. Index codes were added to the libraries to distinguish sequences from each sample. To isolate cDNA fragments selectively, which were 250-300 base pair (bp) long, the library fragments were purified using the AMPure XP system (Beckman Coulter, Inc., Beverly, USA). Subsequently, the size-selected, adaptor-ligated cDNA was treated with 3 μL of the USER Enzyme (New England Biolabs, Inc., USA) at 37 ºC for 15 min, followed by 5 min of incubation at 95 ºC, before prior polymerase chain reaction (PCR). The PCR was conducted using Phusion High-Fidelity DNA polymerase, Universal PCR primers, and Index (X) Primer. The PCR products were purified using the AMPure XP system, and the quality of the library was assessed using the Agilent Bioanalyzer 2100 system (Agilent, USA). The RNA-Seq was carried out on the Illumina HiSeq 150 platform (Illumina, Inc., USA).

Quality Control

To begin, the Fastq-formatted raw data, also known as raw reads, were subjected to processing using Perl scripts. The purpose of this processing step was to obtain clean reads by filtering out reads that contained adapters, poly-N, and low-quality sequences. Furthermore, the clean data's Q20 and Q30 scores, as well as its GC content, were computed. The subsequent analyses were carried out using only high-quality clean data.

Reads Mapping to the Reference Genome

The Human Genome Build GRCh38 reference genome and gene model annotation files were directly obtained from the genome website. The reference genome index was constructed with Spliced Transcripts Alignment to a Reference (STAR) software package version 2.5.1b (National Human Genome Research Institute, USA), and paired-end clean reads were aligned to the reference genome using STAR. STAR utilized the maximal mappable prefix (MMP) approach, which provided an accurate mapping outcome for junction reads.

Quantification of Gene Expression Level

To enumerate the read numbers mapped to each gene, high-throughput sequencing (HTSeq) software package version 0.6.0 (Python, USA) was employed. The Fragments per Kilobase of transcript per Million mapped reads (FPKM) for each gene were then calculated based on its length and the count of mapped reads. FPKM accounts for both sequencing depth and gene length simultaneously and is presently the most widely employed approach for gene estimation.

Gene Ontology (GO) and Reactome Enrichment Analysis of DEGs

The Cluster Profiler R package software package version 4.10.0 (Comprehensive R Archive Network, USA) was utilized to perform GO enrichment and Reactome Pathways analysis of DEGs while accounting for gene length bias. GO enrichments and Reactome Pathways with corrected P value<0.05 were regarded as significantly enriched by DEGs and selected for further downstream analysis.

Protein-protein interaction (PPI) Analysis

Proteins encoded by the common DEGs were used to create a PPI network, which was generated and displayed via the STRING database (https://string-db.org/) and Cytoscape (https://cytoscape.org/). The networks were constructed by extracting the target gene list from the database for the species in question. If unavailable, Blast X software package version 2.2.28 (National Center for Biotechnology Information, USA) aligned the target gene sequences with the reference protein sequences. The networks were built based on the established interaction data of the selected reference species.

Validation of DEGs by qualitative RT-PCR (qRT-PCR) analysis

To validate the upregulated and downregulated DEGs with $\log_2$ FC of ≥2 or ≤-2, qRT-PCR was conducted. Using the RNeasy® Mini Kit (QIAGEN, Germany) and following the manufacturer's guidelines, total RNA was extracted from both DLBCL patients and

healthy volunteers. The RNA was subsequently assessed for concentration and purity using a NanoDrop ND-2000C spectrophotometer (Thermo Scientific, USA). Samples displaying RNA concentrations greater than 10 ng/μL and A260/A280 purity ratios between 1.70 to 2.10 were chosen for qRT-PCR analysis. The qRT-PCR was performed using the Power SYBR® Green RNA-to-CT 1-Step Kit (Applied Biosystems, USA), with a 20 μL reaction volume. The reaction followed the manufacturer's recommended thermal cycling conditions, and the Cycle Threshold (C_t) value was obtained through triplicate samples, utilizing the Applied Biosystems™ 7500 Fast Real-time PCR System machine (Applied Biosystems, USA). The internal control was Glyceraldehyde 3-phosphate dehydrogenase (GAPDH), and the mean± SD based on triplicate experiments was used to present all findings.

Statistical Analysis

For two conditions/groups (with two biological replicates per condition), DEG was conducted using the DESeq2 R package version 1.10.1 (Bioconductor, USA). DESeq2 offers statistical algorithms to identify differential expression in digital gene expression data using a negative binomial distribution model. The obtained P values were corrected with the Benjamin and Hochberg method to control the false discovery rate (FDR), with adjusted P (P_{adj})<0.05 with a $\log_2$ FC of ≥2 or ≤-2 displayed.

The Student's *t* test was utilized to analyze the qRT-PCR data. To assess the likelihood of obtaining the observed outcomes under the null hypothesis, P value statistics were used for analysis. The statistical significance of the observed difference increases as the P value decreases. Results with P<0.05 were regarded as significant.

Results

Assessing Reproducibility of Biological Replicates

To ensure the quality and reproducibility of the RNA-Seq analysis, the data underwent parametric quality control (QC) tests. These tests are essential to increase confidence in the results obtained from the data. The Cluster 3.0 tool was used to plot gene body coverage, correlation matrix, and principal component analysis (PCA). Visualizing the similarities and differences within and between the DLBCL (L2, L3, L4, L5, and L6) and control samples (N1, N2) is crucial to this analysis. Figure 1 shows the PCA of all samples, indicating a strong correlation among them. However, the PCA analysis identified L4 as an outlier from the other DLBCL samples.

Detecting Genes with Differential Expression

By subjecting the transcriptomic data to bioinformatics analysis, significant alterations were identified in 13,679 genes in DLBCL cells compared to controls. Using a FDR threshold of <0.05 and plotting against the $\log_2$ FC≥2 and ≤-2, three upregulated genes and 70 downregulated genes were found (figure 2).

A clustered heat map was utilized to exhibit the expression profiling of DEGs in DLBCL samples relative to control samples. A distinct gene expression pattern in DLBCL samples in contrast to controls was observed by the clustering of the heat map (data not shown).

GO enrichment analysis of DEGs

To gain a better understanding of the potential functions and roles of the identified DEGs in metabolic pathways, they were subjected to gene enrichment analysis. The analysis using GO terms identified 1163 unique groups and pathways. The functional groups of GO groups were determined based on their biological process (BP), molecular function (MF), and cellular component (CC) as identified through the enrichment analysis. Only the GO group with P≤0.05 was considered significant and subsequently chosen for further analysis. Out of 80 significant GO groups, 54 were enriched in BP, 14 in CC, and 12 in molecular functions MF.

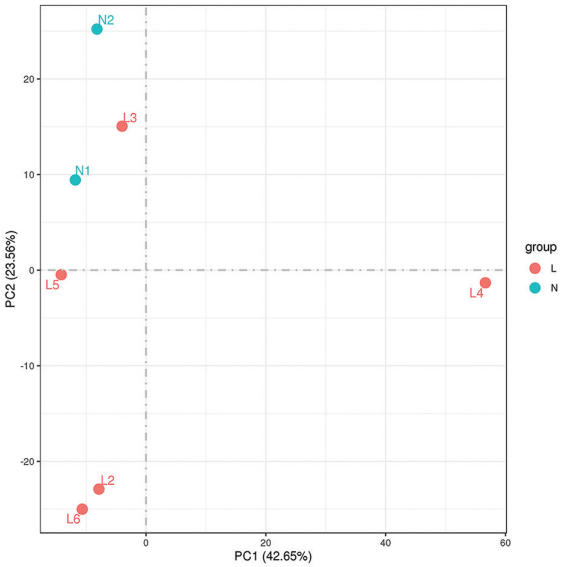

Figure 1: PCA analysis was performed between DLBCL (L2-L6) and control (N1-N2) samples. L: Lymphoma; N: Normal; PC1: Pairwise combination 1; PC2: Pairwise combination 2. PC shows the correlations between the principal components and the original variables based on the PCA formula.

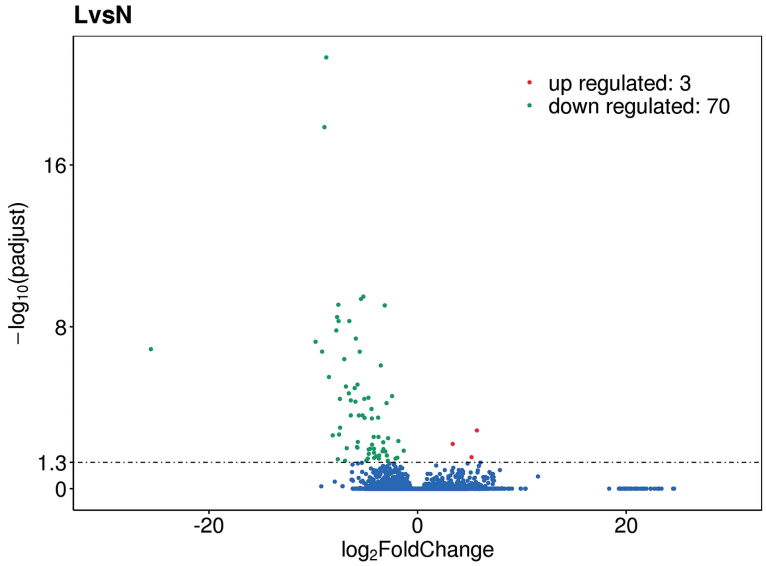

Figure 2: This figure shows a volcano plot of DEGs (FDR<0.05) between DLBCL samples against the normal control samples (LvsN). The horizontal axis is the $\log_2$ fold change between DLBCL and control. The negative log10 of the P value of Fisher's exact test is plotted on the vertical axis. Each gene is represented by one point on the graph. Volcano plot highlights top significant DEGs from DLBCL samples. Significantly upregulated genes are in red; significantly downregulated genes are in green color.

Our results indicated that the frequency of downregulated DEGs was higher than that of upregulated DEGs. In BP, the downregulated DEGs were significantly associated with granulocyte activation (P_{adj}<0.001), neutrophil regulation (P_{adj}<0.001), antimicrobial humoral immune response (P_{adj}<0.001), and cell killing (P_{adj}<0.001) (figure 3), while the upregulated DEGs were significantly correlated with T-cell regulations (P_{adj}<0.001).

As for CC, the DEGs that were downregulated exhibited a marked enrichment in the granule and vesicle lumen (P_{adj}<0.001), while the upregulated DEGs were significantly enriched in the plasma membrane (P_{adj}=0.004), and an extrinsic component of the ribonucleoprotein cytoplasmic side (P_{adj}=0.014).

Subsequently for MF, the downregulated DEGs were significantly associated with chemokine activity and binding (P_{adj}=0.002), G-protein binding (P_{adj}=0.002), oxidoreductase activity, and other protein bindings (P_{adj}=0.026), while the upregulated DEGs were associated with enzyme activities (P_{adj}=0.010).

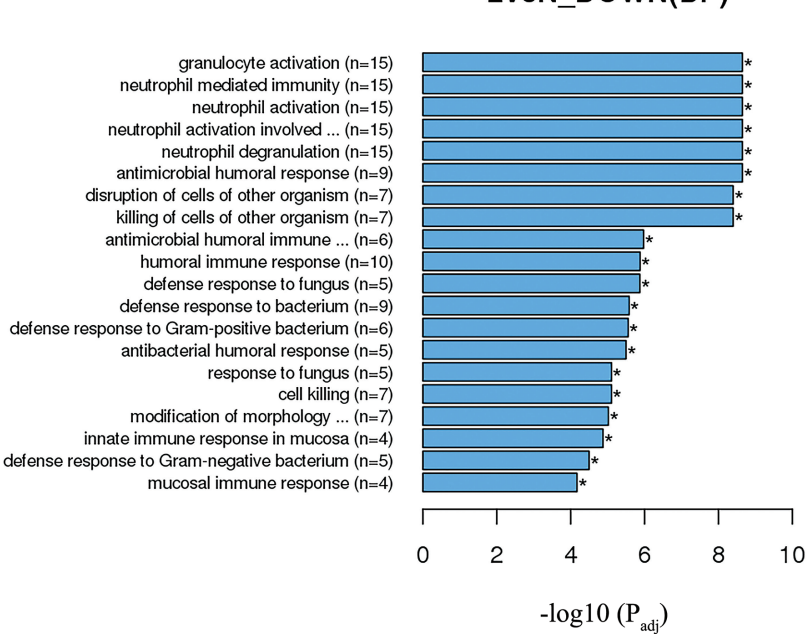

Figure 3: This figure shows the Gene ontology enrichment analysis of DLBCL samples against the normal control samples (LvsN). The enrichment involves BP categories for downregulated genes. *Denotes significant enrichment, P<0.05.

Significantly enriched pathway terms in DEGs

The Reactome pathway analysis was used to determine the pathways that were significantly associated with the identified DEGs from DLBCL samples. To perform downstream analysis, only the GO and Reactome pathways with FDR scores of ≤0.05 were selected. To identify enriched GO and Reactome pathways, a phenotype against genotype analysis was conducted, and statistical significance was determined. Out of 20 Reactome pathways identified, only five were found to be significant, P<0.05 (figure. 4). The findings suggested that DEGs were prominent in several signaling pathways, including antimicrobial humoral response (P_{adj}<0.001), neutrophil degranulation (P_{adj}<0.001), chemokine receptors bind chemokines (P_{adj}=0.028), defensins (P_{adj}=0.028), and metabolism of angiotensinogen (P_{adj}=0.040).

Validation of DEGs by qRT-PCR

To validate the DEGs from the RNA-Seq data, qRT-PCR was conducted. Specifically, we focused on the downregulated DEGs, as they exhibited high significance compared to the upregulated ones. We selected DEGs with a $\log_2$ FC≥2 and ≤-2. The chosen downregulated genes were Cathelicidin antimicrobial peptide (CAMP), Defensin alpha 3 (DEFA3), Defensin alpha 4 (DEFA4), lactotransferrin (LTF), Membrane Spanning 4-Domains A3 (MS4A3), C-C chemokine receptor type 3 (CCR3), CXC chemokine receptor 2 (CXCR2), and CXC chemokine receptor 1 (CXCR1). The qRT-PCR results were consistent with those obtained from RNA-Seq, indicating the reliability and reproducibility of the findings (table 1).

Protein-protein interaction in DLBCL samples

A total of 12 protein pairs involved in DLBCL were identified among the DEGs with a string score of >400. Notably, no pairs were identified among the upregulated DEGs, while 12 pairs were identified among the downregulated DEGs. Table 2 displays the 12 protein pairs with their respective string scores, which illustrates the PPI interaction.

Discussion

While some studies utilize frozen tumor tissue for DLBCL analyses,[7, 8] our approach diverges by employing PBMCs. Unlike frozen tissue, which encompasses all genes in DLBCL, our study specifically targets immune-associated cells.

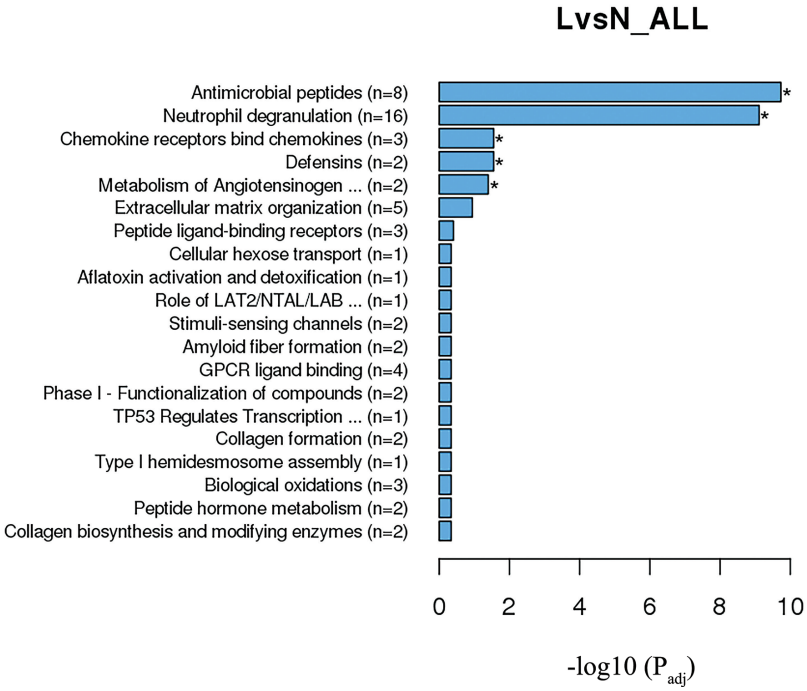

Figure 4: This figure shows Reactome enrichment analysis for DLBCL samples against the normal control samples (LvsN). *Denotes significant enrichment analysis, P<0.05.

Table 1: Validation of qRT-PCR analysis on genes listed above

Genes	CAMP	MS4A3	LTF	CCR3	DEFA3	DEF4A	CXCR2	CXCR1
Fold change expression	-1.51***	-1.2**	-1.6***	-1.03	-1.12**	-1.19	-1.09	-1.32***

The P values were determined using Student's *t* test and are indicated in the table. Significance levels were set at P<0.05. The qRT-PCR results are in agreement with the RNA-Seq data. The P<0.05 were considered significant. Significance levels were labeled as **P<0.01, ***P<0.001.

Table 2: The 12 protein pairs in the string score

Node 1 name	Node 1 protein	Node 2 name	Node 2 protein	Score
CEACAM6	9606.ENSP00000199764	CEACAM8	9606.ENSP00000244336	970
CTSG	9606.ENSP00000216336	CPA3	9606.ENSP00000296046	428
CTSG	9606.ENSP00000216336	DEFA3	9606.ENSP00000328359	506
LTF	9606.ENSP00000231751	TCN1	9606.ENSP00000257264	660
LTF	9606.ENSP00000231751	LCN2	9606.ENSP00000277480	414
CHI3L1	9606.ENSP00000255409	LCN2	9606.ENSP00000277480	416
TCN1	9606.ENSP00000257264	MS4A2	9606.ENSP00000278888	610
CXCR1	9606.ENSP00000295683	CXCR2	9606.ENSP00000319635	956
CXCR1	9606.ENSP00000295683	CCR3	9606.ENSP00000441600	918
CPA3	9606.ENSP00000296046	GATA2	9606.ENSP00000345681	448
DEFA4	9606.ENSP00000297435	DEFA3	9606.ENSP00000328359	907
CXCR2	9606.ENSP00000319635	CCR3	9606.ENSP00000441600	918

This table shows the 12 protein pairs for DEGs that are involved in DLBCL (string score>400). For the upregulated DEGs, 0 pairs were identified, while 12 pairs were identified for downregulated DEGs

This distinction is crucial as our research zeroes in on the immune aspects of DLBCL, emphasizing the tumor microenvironment. In contrast to studies concentrating on long non-coding RNA[9] and miRNA,[8] there is a noticeable gap in the literature concerning PBMC-focused investigations in DLBCL. Nevertheless, there are some studies that focus on immune infiltrates within cancer cells to represent the immune microenvironment *in situ*.[7, 8] However, this method has limitations. It is inherently more difficult for obtaining the samples due to the invasive nature of the surgery and the challenges in taking repeated sampling. Our approach using PBMCs not only addresses these logistical challenges but also offers a patient-friendly avenue for continuous monitoring, allowing for a more comprehensive understanding of the dynamic immune landscape in DLBCL. This accessibility not only streamlines the diagnostic process but also facilitates ongoing monitoring of treatment regimes. The ability to obtain samples at different time points allows for a dynamic assessment of immune responses during the course of treatment, offering valuable insights for personalized and real-time therapeutic adjustments.

Due to distinct focuses and variations in sampling methodologies, the results are not directly comparable. To the best of our knowledge, not many studies have specifically utilized PBMCs in the investigation of DLBCL using RNA-Seq. Nonetheless, the common findings among most of the studies including ours, indicate significant differences in the inflammatory responses, tumor-cell dissemination, tumor suppressor gene expression, and cell cycle.[7, 8]

In our study, a significant decrease in the antimicrobial humoral response in tumor samples was observed. One of the key players in this response is the CAMP, which not only exhibits antibacterial, antifungal, and antiviral activities but also regulates inflammatory responses and tissue repair, acting via neutrophil N-formyl peptide receptors to enhance the release of chemokine C-X-C motif ligand 2 (CXCL2).[10] Thus, significant downregulation of CAMP may lead to a reduction in inflammatory responses and downstream pathways that are involved in eliminating cancer cells. This effect is supported by the downregulated genes in neutrophil degranulation and neutrophil degranulation. These findings suggest that there is a downregulation in neutrophil degranulation and inflammation in tumor samples, which may contribute to the progression of DLBCL.

Defensins are peptides with cytotoxic properties that contribute to host defense and display antimicrobial activity. They are highly abundant in neutrophils.[10] DEFA3 is involved in phagocyte-mediated host defense, while DEFA4 is primarily found in neutrophils. The downregulation of defensin expression in DLBCL patients is likely to affect the function and mechanism of neutrophil degranulation and inflammation in tumor samples, ultimately contributing to the progression of DLBCL cancer.

LTF plays a significant role in regulating cellular growth, differentiation, and protection against cancer development and metastasis in various cancers.[11] It exhibits anti-tumor and anti-metastatic properties.[12] In the context of DLBCL, the downregulation of LTF removes its anti-tumor effects and attenuates capabilities toward cell growth and invasion. This allows DLBCL cells to proliferate and invade, leading to cancer development and metastasis. This study suggests that LTF is a potential therapeutic target for DLBCL and other cancers.

The MS4A3 plays a role in modulating the G1-S cell cycle transition in hematopoietic cells by directly binding to cyclin-dependent kinase

(CDK) inhibitor 3 and altering the phosphorylation level of CDK-2, in addition to its function in LTF.[13] The downregulation of MS4A3 in DLBCL cells suggests the removal of negative regulation on the cell cycle and consequent upregulation of the G1-S cell cycle transition. This supports the cancer cells growth and metastasis.

The increase in the numbers of downregulated genes associated with the chemokine-mediated signaling pathway as well as the CCR and CXCR activities imply a decrease in the responsiveness and function of chemokines in the tumor samples.

CCR3 serves as a receptor for C-C-type chemokines, binding and responding to various chemokines such as eotaxin (CCL11), eotaxin-3 (CCL26), monocyte chemotactic protein-3 (MCP3) also known as CCL7, monocyte chemoattractant protein (MCP4) also known as CCL13, RANTES (CCL5), and chemokine (C-C motif) ligand 15 (CCL15).[14] This receptor is highly expressed in eosinophils and basophils[15] and is also detected in Type 1 T helper cells (Th1) and Type 2 T helper cells (Th2).[16] CCR3 likely plays a role in the accumulation and activation of eosinophils and other inflammatory cells. Suppression of CCR3 results in reduced activity of chemokine binding and activation of inflammatory cells.

CXCR1 and CXCR2 act as receptors for Interleukin-8 (IL-8), which is a potent chemotactic factor for neutrophils.[17, 18] The binding of IL-8 to these receptors leads to neutrophil activation, which occurs through a G-protein that activates a phosphatidylinositol-calcium second messenger system.[19] Since IL-8 involves high affinity binding, downregulation of CXCR1 and CXCR2 reduces the activity of IL-8 binding and neutrophil activation. In protein-protein analysis, these three chemokine receptor genes (CCR3, CXCR1, and CXCR2) interact well and possibly result in the downregulation of the chemokine response and neutrophil activation in DLBCL patients.

The constraints of our study stem from a small sample size and restricted funding, preventing the analysis of larger sample sizes through sequencing. With the limited sample size, there is a potential for certain genes to be excluded due to constraints in statistical significance.

Conclusion

The findings of this study demonstrate the identification of 73 DEGs between DLBCL patients and control samples. The downregulation of antimicrobial humoral response, neutrophil degranulation and activation, chemokines response, and defensins pathways in DLBCL patients, suggest that these pathways may contribute to cancer progression and poor immune response in affected individuals. These may serve as potential targets for DLBCL treatment and contribute to understanding target genes and pathways involved in DLBCL.

Acknowledgment

The Ministry of Higher Education Malaysia supported the project, grant ID: FRGS/1/2017/SKK08/UKM/03/2; data analysis was supported by industry grant Codon Genomics CoGen Insights Grant, grant ID: COGEN/IGNITE/2021/07 & JJ-2022-002; publication of the article was supported by GP-K019325. We also thank Mohd Razif Mohd Idris and Nor Azimah Ismail (Cell Therapy Center, HTCM), for assisting in sample collection.

Authors' Contribution

N.A.J., H.Z.M.S., and W.F.WJ: conception and design of the study; N.A.J., A.S., and W.K.L: acquisition, analysis, and interpretation of data. All authors drafted and reviewed the manuscript critically. All authors have read and approved the final manuscript and agree to be accountable for all aspects of the work in ensuring that questions related to the accuracy or integrity of any part of the work are appropriately investigated and resolved.

Conflict of Interest: None declared.

References

1 Sung H, Ferlay J, Siegel RL, Laversanne M, Soerjomataram I, Jemal A, et al. Global Cancer Statistics 2020: GLOBOCAN Estimates of Incidence and Mortality Worldwide for 36 Cancers in 185 Countries. CA Cancer J Clin. 2021;71:209-49. doi: 10.3322/caac.21660. PubMed PMID: 33538338.

2 Satou A, Bennani NN, Feldman AL. Update on the classification of T-cell lymphomas, Hodgkin lymphomas, and histiocytic/dendritic cell neoplasms. Expert Rev Hematol. 2019;12:833-43. doi: 10.1080/17474086.2019.1647777. PubMed PMID: 31365276; PubMed Central PMCID: PMCPMC6763378.

3 Poletto S, Novo M, Paruzzo L, Frascione PMM, Vitolo U. Treatment strategies for patients with diffuse large B-cell lymphoma. Cancer Treat Rev. 2022;110:102443. doi: 10.1016/j.ctrv.2022.102443. PubMed PMID: 35933930.

4 Sawalha Y. Relapsed/Refractory Diffuse Large B-Cell Lymphoma: A Look at the Approved and Emerging Therapies. J Pers Med. 2021;11. doi: 10.3390/jpm11121345. PubMed PMID: 34945817; PubMed Central PMCID: PMCPMC8708171.
5 Hong M, Tao S, Zhang L, Diao LT, Huang X, Huang S, et al. RNA sequencing: new technologies and applications in cancer research. J Hematol Oncol. 2020;13:166. doi: 10.1186/s13045-020-01005-x. PubMed PMID: 33276803; PubMed Central PMCID: PMCPMC7716291.
6 Peymani F, Farzeen A, Prokisch H. RNA sequencing role and application in clinical diagnostic. Pediatr Investig. 2022;6:29-35. doi: 10.1002/ped4.12314. PubMed PMID: 35382420; PubMed Central PMCID: PMCPMC8960934.
7 Serrano Lopez J, Jimenez-Jimenez C, Chutipongtanate S, Serrano J, Rodriguez-Moreno M, Jimenez A, et al. High-throughput RNA sequencing transcriptome analysis of ABC-DLBCL reveals several tumor evasion strategies. Leuk Lymphoma. 2022;63:1861-70. doi: 10.1080/10428194.2022.2056173. PubMed PMID: 35379068.
8 Sheng L, Fu D, Cao Y, Huo Y, Wang S, Shen R, et al. Integrated Genomic and Transcriptomic Analyses of Diffuse Large B-Cell Lymphoma With Multiple Abnormal Immunologic Markers. Front Oncol. 2022;12:790720. doi: 10.3389/fonc.2022.790720. PubMed PMID: 35237512; PubMed Central PMCID: PMCPMC8882913.
9 Zhou M, Zhao H, Xu W, Bao S, Cheng L, Sun J. Discovery and validation of immune-associated long non-coding RNA biomarkers associated with clinically molecular subtype and prognosis in diffuse large B cell lymphoma. Mol Cancer. 2017;16:16. doi: 10.1186/s12943-017-0580-4. PubMed PMID: 28103885; PubMed Central PMCID: PMCPMC5248456.
10 Xu D, Lu W. Defensins: A Double-Edged Sword in Host Immunity. Front Immunol. 2020;11:764. doi: 10.3389/fimmu.2020.00764. PubMed PMID: 32457744; PubMed Central PMCID: PMCPMC7224315.
11 Xiong S, Dong L, Cheng L. Neutrophils in cancer carcinogenesis and metastasis. J Hematol Oncol. 2021;14:173. doi: 10.1186/s13045-021-01187-y. PubMed PMID: 34674757; PubMed Central PMCID: PMCPMC8529570.
12 Li WY, Li QW, Han ZS, Jiang ZL, Yang H, Li J, et al. Growth suppression effects of recombinant adenovirus expressing human lactoferrin on cervical cancer in vitro and in vivo. Cancer Biother Radiopharm. 2011;26:477-83. doi: 10.1089/cbr.2010.0937. PubMed PMID: 21834714.
13 Kutok JL, Yang X, Folkerth R, Adra CN. Characterization of the expression of HTm4 (MS4A3), a cell cycle regulator, in human peripheral blood cells and normal and malignant tissues. J Cell Mol Med. 2011;15:86-93. doi: 10.1111/j.1582-4934.2009.00925.x. PubMed PMID: 19818099; PubMed Central PMCID: PMCPMC3822496.
14 Zhang L, Soares MP, Guan Y, Matheravidathu S, Wnek R, Johnson KE, et al. Functional expression and characterization of macaque C-C chemokine receptor 3 (CCR3) and generation of potent antagonistic anti-macaque CCR3 monoclonal antibodies. J Biol Chem. 2002;277:33799-810. doi: 10.1074/jbc.M205488200. PubMed PMID: 12101185.
15 Stellato C, Brummet ME, Plitt JR, Shahabuddin S, Baroody FM, Liu MC, et al. Expression of the C-C chemokine receptor CCR3 in human airway epithelial cells. J Immunol. 2001;166:1457-61. doi: 10.4049/jimmunol.166.3.1457. PubMed PMID: 11160184.
16 Yuan J, Liu Y, Yu J, Dai M, Zhu Y, Bao Y, et al. Gene knockdown of CCR3 reduces eosinophilic inflammation and the Th2 immune response by inhibiting the PI3K/AKT pathway in allergic rhinitis mice. Sci Rep. 2022;12:5411. doi: 10.1038/s41598-022-09467-4. PubMed PMID: 35354939; PubMed Central PMCID: PMCPMC8969185.
17 Capucetti A, Albano F, Bonecchi R. Multiple Roles for Chemokines in Neutrophil Biology. Front Immunol. 2020;11:1259. doi: 10.3389/fimmu.2020.01259. PubMed PMID: 32733442; PubMed Central PMCID: PMCPMC7363767.
18 Park SH, Das BB, Casagrande F, Tian Y, Nothnagel HJ, Chu M, et al. Structure of the chemokine receptor CXCR1 in phospholipid bilayers. Nature. 2012;491:779-83. doi: 10.1038/nature11580. PubMed PMID: 23086146; PubMed Central PMCID: PMCPMC3700570.
19 Lomakina EB, Waugh RE. Signaling and Dynamics of Activation of LFA-1 and Mac-1 by Immobilized IL-8. Cell Mol Bioeng. 2010;3:106-16. doi: 10.1007/s12195-009-0099-x. PubMed PMID: 21532911; PubMed Central PMCID: PMCPMC3084010.